PHYSICAL REVIEW B **92**, 014502 (2015)

Questioning the existence of superconducting potassium doped phases for aromatic hydrocarbons

Satoshi Heguri,[1,*] Mototada Kobayashi,[2,*] and Katsumi Tanigaki[1,3,*]

[1]*World Premier International Research Center Initiative Advanced Institute for Materials Research (WPI-AIMR), Tohoku University, 2-1-1 Katahira, Aoba-ku, Sendai 980-8577, Japan*

[2]*Graduate School of Material Science, University of Hyogo, 3-2-1 Kouto, Kamigohri, Hyogo 678-1297, Japan*

[3]*Graduate School of Science, Tohoku University, 6-3 Aramaki, Aoba-ku, Sendai 980-8578, Japan*

(Received 30 May 2015; published 7 July 2015)

Superconductivity in aromatic hydrocarbons doped with potassium (K) such as K_3 [picene (PCN)] and K_3 [phenanthrene (PHN)] is found for only armchair-type polycyclic aromatic hydrocarbon. In this paper the thermodynamics of the reaction processes of PHN or anthracene (AN, zigzag type) with K was studied using differential scanning calorimetry and x-ray diffraction. We show that PHN decomposes during the reaction, triggered by hydrogen abstraction, to give metal hydride KH and unknown amorphous. No stable doped phases exist in K_x(PHN) with stoichiometries of $x = 1$–3. However, in the case of AN, a stable doped phase forms. We claim that PHN, which has been reported to be energetically more stable in the ground state than AN by first principle calculations, is unstable upon doping. We also suggest that the superconductivity in K_3(PCN) is due to the misinterpretation of experimental data, which actually arises from ferromagnetic impurities. We have never detected the superconductivity above 2 K in these compounds. The superconductivity in both K_x(PHN) and K_x(PCN) is concluded to be highly questionable.

DOI: 10.1103/PhysRevB.92.014502 PACS number(s): 74.70.Kn, 82.20.−w, 82.60.Hc, 74.72.Ek

I. INTRODUCTION

Since alkali metal doped polycyclic aromatic hydrocarbons (PAHs), picene ($C_{22}H_{14}$; PCN) [1] and phenanthrene ($C_{14}H_{10}$; PHN) [2] were reported to exhibit superconductivity, various electronic properties of these superconductors, such as electron-phonon interactions and electron correlations competing between itineration and localization of electrons, have been reported [3–10]. On the other hand, few experimental studies regarding these findings have been reported, and many controversies remain [11,12]. In the case of the photoemission spectroscopic studies reported by three research groups, two research groups have reported that they are not metallic because there is no Fermi edge in the spectra, whereas one group, the same research group that originally reported that K doped picene is a superconductor, reported evidence for the existence of metallic states for K_x(PCN) films [13–16]. Raman spectroscopy has been used to characterize the superconducting phase; however, such discussions are not valid because the superconducting shielding fraction is generally less than 1% and the dominant phases detected in Raman are not superconducting [11,12,17,18].

In this metal doped system, superconductivity has been observed only for armchair-type PAHs, and no superconductivity has been observed for zigzag-type ones. Isostructural geometries are frequently the center of interest for the case of organic materials because molecules containing asymmetric carbon atoms are chiral and because nonsuperimposable isomers often exist in nature and are important from a pharmaceutical viewpoint. Moreover, *cis*- and *trans*-geometrical isomers frequently have different catalytic abilities. For example, polybutadiene, which has contributed significantly to industry in the past, is made from the *trans*-isomer [19]. In the case of graphene, an infinitely large density of states at the Fermi level along with spin ordering has been theoretically predicted only for the graphite ribbon with a zigzag edge [20,21], and the experimental observation of such electronic states is presently a research topic of top priority. Thus, the superconductivity of K doped PAHs is an intriguing issue to be discussed, namely, why only armchair-type PAHs show superconductivity.

In this paper we examine the reaction processes of two structural isomers containing three benzene rings, PHN and anthracene (AN), by employing differential scanning calorimetry (DSC) and x-ray diffraction (XRD), from the viewpoint of their thermodynamic properties. In the DSC traces for both PHN and AN, endothermic peaks associated with a phase transition from a solid to a liquid, which correspond to the melting point of each starting material, and exothermic peaks originating from a chemical reaction with K are observed only at temperatures above 550 K. In the XRD profiles for the stoichiometric composition corresponding to K_3 (PHN), peaks from KH and unknown phases are observed at high angles, indicating that molecular decomposition occurs in PHN. Our experimental observations are significantly different from those of previous report on PHN, in which they reported the formation of a doped phase [2]. In contrast, intriguingly in the case of AN, diffraction peaks associated with a doped phase are observed, although no superconductivity is detected. These comparative studies between PHN and AN clearly show that doping using K metal is thermodynamically impossible for PHN, and hence that the metallic phase, let alone superconductivity, of K_x(PHN), is highly doubtful. In addition to PHN, PCN, which has been reported to show superconductivity, is claimed not to show any superconductivity. It is also pointed out that PHN and PCN with alkaline earth and rare earth metals do not react below the melting point of PAHs.

II. EXPERIMENTAL

Sublimed PHN (over 99.5% purity), AN (over 99.0% purity), K metal (99.5% purity), Ca metal

*Corresponding authors: heguri@sspns.phys.tohoku.ac.jp; kobayasi@sci.u-hyogo.ac.jp; tanigaki@sspns.phys.tohoku.ac.jp

(99.9% purity), Sr metal (99.9% purity), La metal (99.9% purity), and Sm metal (99.9% purity) were purchased from Sigma-Aldrich. Sublimed PCN (99.9% purity) was purchased from NARD. PHN was purified again by using a conventional sublimation technique prior to use. The surfaces of the metal ingots were cleaved in an argon (Ar) glove box (O_2, 0.1 ppm) in order to remove the oxidized surface. The purified PAHs were mixed carefully with nonoxidized pure K ingots with the chemical stoichiometries of K_x (PHN/AN/PCN) ($x = 1$–3). The mixtures were then sealed into a quartz tube with helium (He) gas after evacuation. The samples were thermally treated at several conditions in an electric furnace.

DSC measurements were performed on a Rigaku Thermo plus EVO2 DSC8230 system using powder samples (~8 mg). They were pristine materials, and their mixtures with metals or metal were loaded into stainless steel (SS) sample pans, and the sample pans were hermetically sealed using aluminum covers. The samples were heated in a flow of pure Ar gas at a rate of 5 K/min up to 600 K. There were no evidence for reactions between metals and the SS hermetically sealed pan up to 600 K. The crystal structures were investigated by using powder XRD measurements at room temperature on a Rigaku SmartLab equipped with a monochromator, a Cu rotating-anode generator, and a high-speed position sensitive detector. For the annealing time dependence of XRD profiles, the mixtures were sealed in quartz capillaries under a He atmosphere, the tubes were subsequently annealed at reported conditions, and then the measurements were performed without exposure to air. The K-PHN/AN/PCN specimens were sealed in hand-made quartz tubes with He gas used for thermal exchange. Magnetization measurements were carried out under an applied magnetic field (H) of 10 Oe or 5 Oe on a Quantum Design MPMS-XL7, −7, or −5 superconducting quantum interference device (SQUID) magnetometer.

III. RESULTS AND DISCUSSION

A. Reaction processes in PHN and AN with K

Thermodynamic properties of reaction processes can be monitored using DSC, and a similar method was applied to study the C_{60} with alkali metals by Chen *et al.* [22]. We employed the same technique to investigate the reaction of PHN and AN with K. Typical DSC traces are shown in Fig. 1. In the spectra of both pristine PHN and AN, clear endothermic peaks were observed around 373 K and 491 K [Figs. 1(e) and 1(c)], respectively, and these peaks correspond to the melting points of PHN and AN. When we repeated the same experiments for PHN or AN with K, an additional endothermic peak attributed to the melting point of K metal was detected at 336 K. In addition, a few broad exothermic peaks at high temperatures (>500 K) were observed in the DSC traces for both samples of PHN and AN with K [Figs. 1(d) and 1(b)]. For reference, we studied C_{60} mixed with K using DSC (Fig. 2), and a clear exothermic peak appeared at ~336 K, which is the temperature as the melting point of K. At higher temperatures, broad peaks were observed, as has been reported previously [22]. These broad peaks are indicative of the formation of various stable

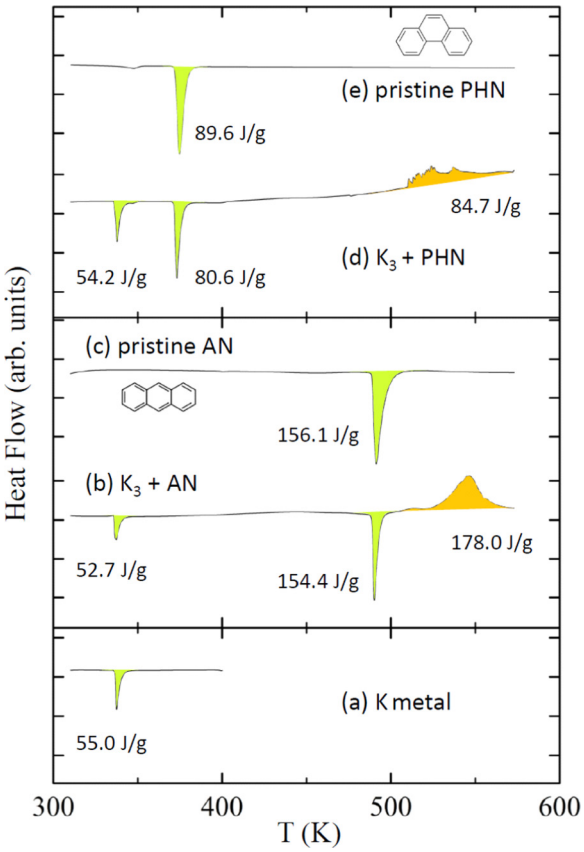

FIG. 1. (Color online) Typical DSC traces for (a) K metal, (b) K_3+AN, (c) pristine AN, (d) K_3+PHN, and (e) pristine PHN.

phases of the fullerides: K_1C_{60}, K_3C_{60}, K_4C_{60}, and K_6C_{60} as the line compounds. These experimental results suggest that the reaction, which provides stabilization energy, is initiated immediately after the K metal melts. On the other hand, relatively small endothermic peaks were detected in DSC for both PHN and AN at the melting point of K metal, indicating that only small changes occur in the cases of PHN and AN. Moreover, the exothermic peak observed for AN was more

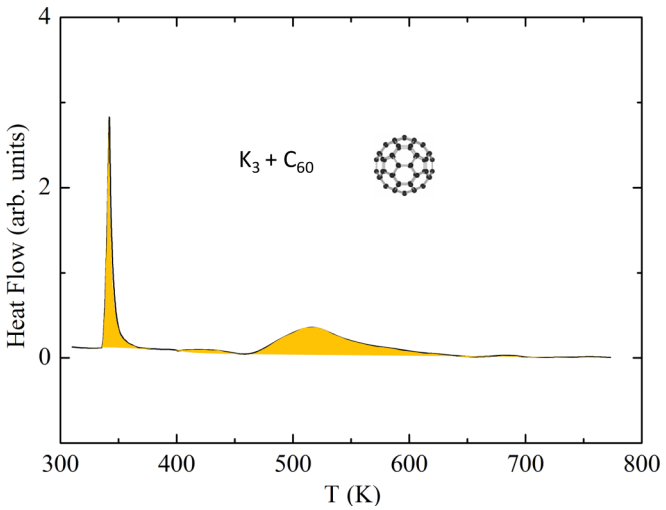

FIG. 2. (Color online) DSC trace for K_3+C_{60}.

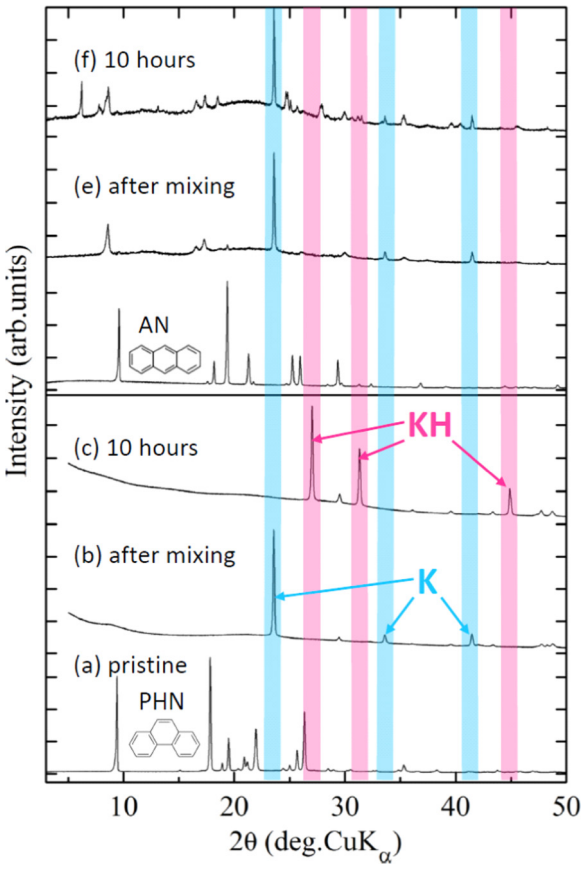

FIG. 3. (Color online) Annealing time dependence of XRD profiles for (a)–(c) K_3+PHN and (d)–(f) K_3+AN compounds. (a) Pristine, (b, e) after mixing, and (c, d) annealing time of 10 h. The red and blue lines correspond to the peak positions of KH and free K, respectively.

apparent than that for PHN [Figs. 1(b) and 1(d)]. The details of phase formation are discussed in connection to the XRD studies in the next paragraph. In order to understand the reaction process of PHN and AN with K, the annealing time dependences were studied by using XRD (Fig. 3). The XRD profile of the starting PHN was indexed to its monoclinic structure: $a = 8.460$, $b = 6.155$, $c = 9.458$ Å, and $\beta = 98.0°$. The diffraction peaks of pristine AN were indexed to the monoclinic structure: $a = 8.556$, $b = 6.016$, $c = 11.176$ Å, $\beta = 124.5°$. These crystal structures are consistent with those in previous papers [23,24]. Pristine PHN and AN were mixed with K in a stoichiometry of 1:3, and then the samples were annealed. After annealing, the changes in crystal structures were sequentially monitored by using XRD. We observed morphological changes indicative of reactions solely involving mechanical grinding even at room temperature, although additional annealing at a higher temperature was necessary to complete the phase stabilization.

The original peaks assigned to the pristine PHN almost completely disappeared after annealing, and several new peaks appeared, as shown in Fig. 3(b). Rietveld refinement was carried out on the XRD profiles [Fig. 4(a)], and the new peaks were indexed to free K metal while ignoring a few unknown peaks. The results suggest that the PHN crystal becomes amorphous during mechanical grinding with K. A phase-separated mixture of K fine powder and miscellaneous carbons were observed by using an optical microscope, showing that the reaction with K was not complete. Peaks for free K metal and for unknown phases were also detected in XRD profiles. When we roughly estimated the amount of K and PHN using the original stoichiometry of 3 to 1, their volumes were nearly comparable. In other words, careful grinding at temperatures lower than the melting point does not induce sufficient reaction of PHN with K. After a reaction time of 10 h at 473 K, the sample color changed from gray to black. In addition, the XRD profile changed [Fig. 3(c)], and peaks appeared at higher diffraction angles than those observed immediately after mixing. Finally, the peaks corresponding to the parent PHN and free K metal were no longer observed. The XRD profile of the sample annealed for 20 h was similar to that after 10 h of annealing (Fig. 5). This fact indicates that the reaction is complete after annealing for 10 h. Figure 4(b) shows the Rietveld refinement of the XRD profile for the sample annealed for 20 h. The main peaks were assigned to those for KH and unidentifiable by-products. The small broad peaks at $2\theta \approx 20°$ are due to an amorphous phase that formed upon decomposition of PHN. The formation of KH indicates that the decomposition of the PHN molecules is triggered by hydrogen abstraction by the K elements.

As for K-AN, intriguingly in contrast to the K-PHN system, sharp peaks corresponding to free K metal were detected after mixing, and new diffraction peaks appeared at diffraction angles lower than the lowest angle of the diffraction peaks for pristine AN, as shown Fig. 3(e). This indicates that the observed diffraction profiles are due to a doped phase with lattice expansion upon insertion of K into the space of the van der Waals crystal, which is frequently observed for metal doped molecular crystals. After heating for 5 h, not only the appearance of many new peaks but also the disappearance of diffraction peaks derived from the pristine AN were observed (Fig. 6), suggesting that a reaction proceeded without decomposition of AN. Recently we have reported that K doped AN with the 1:1 stoichiometry in bulk K_1(AN) is a Mott insulator, which fully explains its optical and magnetic properties, whereas K_2(AN) is a band insulator [25,26]. Since K_1(AN) and K_2 (AN) are stable phases, it is reasonable that K remains after the reactions because a stoichiometry of 3:1 was initially used. The XRD profile after 20 h of annealing was similar to that after 10 h of annealing (Fig. 5). In other words, the reaction was complete after 10 h of annealing, which is similar to the case of K_3+PHN. Diffraction peaks for KH were not detected in the profiles for K_3+AN. The reactivity of PHN or AN with K is opposite to what was expected from the stabilities of their molecular structures in the ground states [17,27].

Le Bail analysis was performed on the XRD profile after 20 h of annealing to obtain the lattice parameters for K_3+AN (Fig. 7). Almost all peaks were indexed for a doped phase with a triclinic cell, and the lattice parameters were determined to be $a = 11.970$, $b = 15.375$, $c = 10.571$ Å, $\alpha = 103.31°$, $\beta = 97.96°$, and $\gamma = 71.26°$. This lattice volume is about twice that of pristine AN. These preliminary analyses imply that the doped K ions randomly occupy both inter- and intralayers of the AN molecules, indicating a disordered

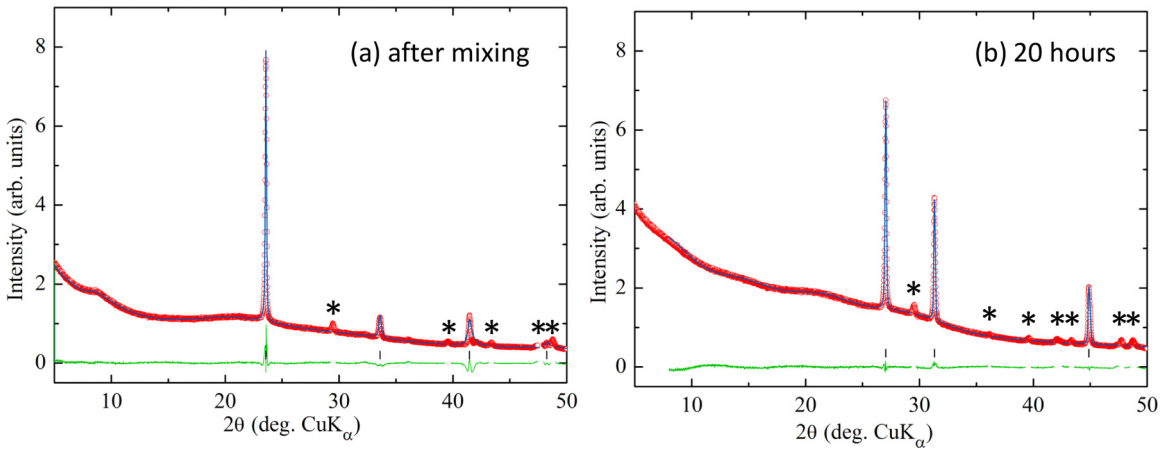

FIG. 4. (Color online) XRD profiles for (a) K_3+PHN immediately after mixing, and (b) K_3+PHN after 20 h of annealing. Powder XRD profiles at ambient temperature, red circles. Blue lines were calculated. The lower green solid line shows the differences between the calculated and observed profiles, and the tick marks indicate the reflection position of (a) free K metal and (b) KH. Asterisks (*) indicate unidentified peaks. Rietveld refinements were carried out by excluding the unidentified peaks.

structure. This is a common problem for metal doped PAHs, i.e., the existence of other stoichiometries and/or polymorphic phases, and therefore the interpretation of XRD profiles becomes extremely difficult. In fact, further refinement of our data is needed for detailed discussion. Accurate crystal structural determination of low-dimensional structures, like metal doped PAHs, is an ongoing and important challenge, and the crystal structure determination of doped C_{60} by using Rietveld refinement was successful only because of the high symmetry of the molecule.

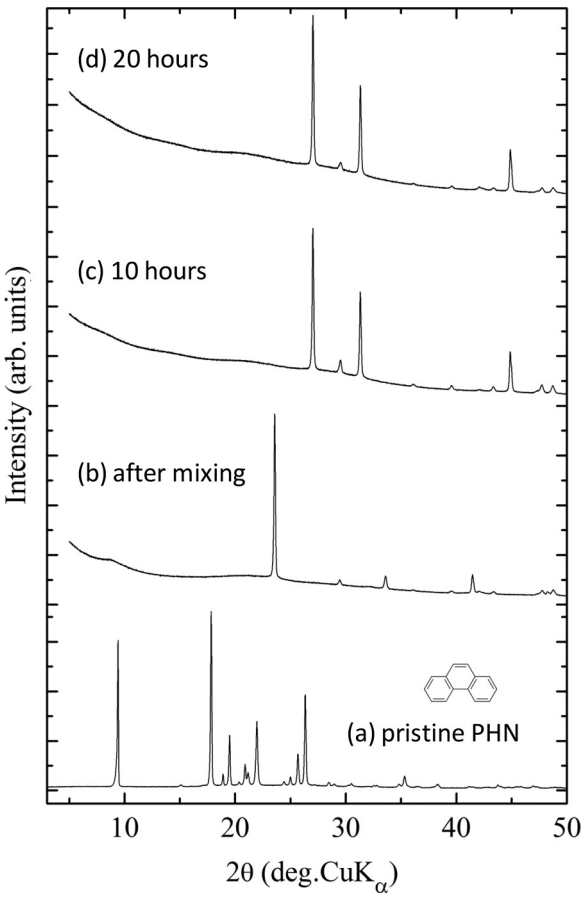

FIG. 5. Annealing time dependence of XRD profiles for K-PHN compound: (a) pristine PHN, (b) immediately after mixing of K_3+PHN, (c) after 10 h of annealing, and (d) after 20 h of annealing.

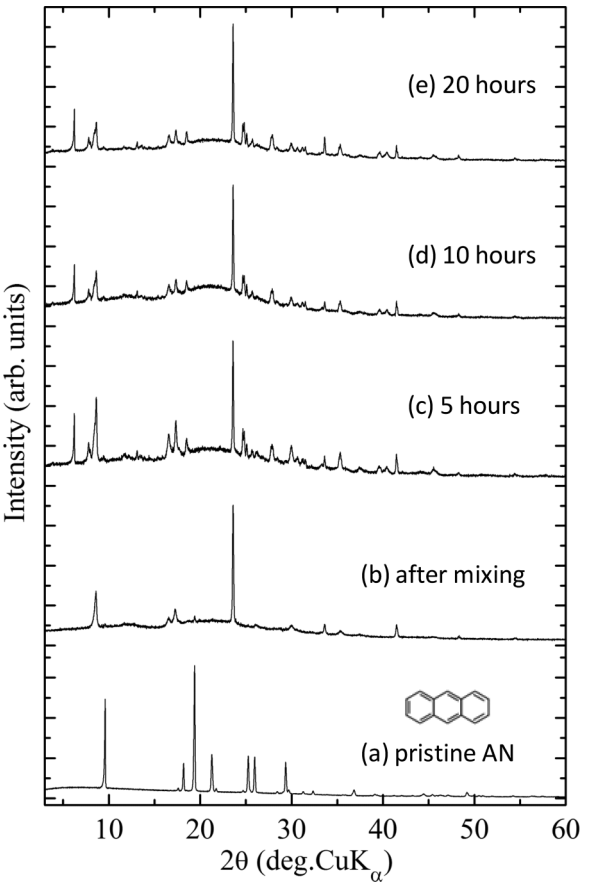

FIG. 6. Annealing time dependence of XRD profiles for K-AN compound: (a) pristine AN, (b) immediately after mixing, (c)–(e) after 5, 10, and 20 h annealing, respectively.

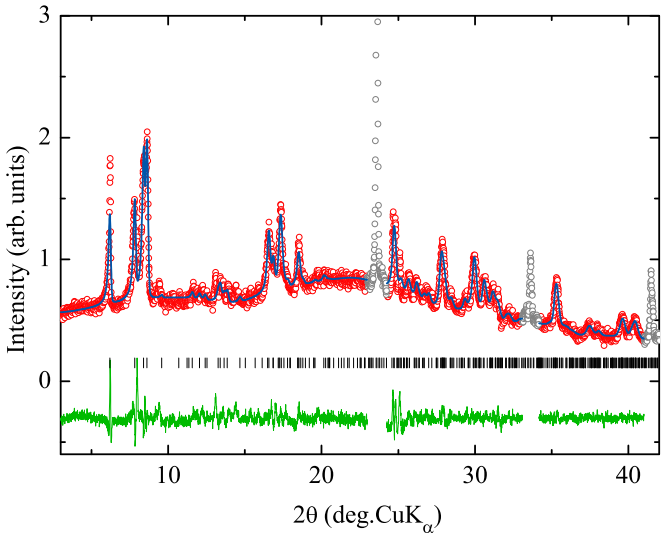

FIG. 7. (Color online) Le Bail analysis on the XRD profile of K-AN after 20 h of annealing. Observed (red and gray circles) and calculated (blue solid line) powder XRD profiles at ambient temperature. The lower green solid line shows the differences between the observed and calculated profile, and the tick marks indicate the allowed reflection positions for the intercalation phase. The analysis was carried out excluding the free K metal peaks (gray circles).

From the XRD data, it is clearly known that the K-AN system has a stable doped phase, whereas the K-PHN does not have a stable one, although K_3 (PHN) was reported to be a stable phase in a previous paper [2]. For further confirmation of the electronic states, we prepared K_x (PHN) with $x = 1$–3 and measured their magnetic properties to investigate the occurrence of superconductivity. The temperature dependence of the magnetic susceptibilities was measured under an applied magnetic field (H) of 10 Oe. In zero field cooling (ZFC) measurements, even a trace of the diamagnetic signal associated with superconductivity was not observed (Fig. 8).

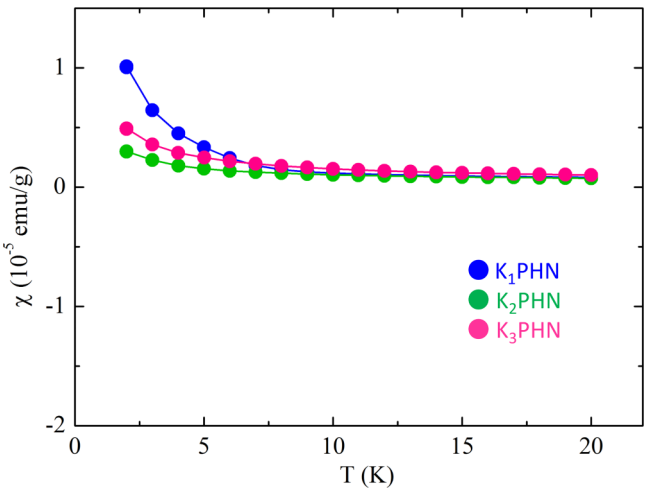

FIG. 8. (Color online) Temperature dependence of the magnetic susceptibility of K_xPHN [$x = 1$ (blue), 2 (green), 3 (red)]. Samples were annealed at 473 K for 20 h, following the procedure in the previous report.

The magnetic susceptibilities of the samples increased with a decrease in temperature, which is indicative of Curie paramagnetic behavior. No signals associated with superconductivity were observed for more than 60 samples prepared in our laboratory. The superconductivity observed previously for the K-PHN system [2] is highly questionable.

B. Thermodynamics of PHN with alkaline earth and rare earth metal

Almost all PAH superconductors have been reported to show a very small superconducting shielding fraction. Although a high superconducting shielding fraction of 65% was once reported for alkaline earth metal doped PHN, $Ba_{1.5}$ (PHN) [28], recent thermodynamic studies have definitely claimed that this result is questionable [29]. In the case of rare earth metals, superconductivity was also reported for PHN [30,31]. In order to clear the situation, thermograms of PHN with Sr, Sm, or La were measured, but only endothermic peaks associated with a solid-liquid phase transition of pristine PHN were observed (Fig. 9). These DSC measurements clearly indicate that no reactions occur in PHN with Sr, Sm, or La at annealing temperatures below their melting points. This is scientifically reasonable because the activation energy of these elements for reaction is much larger than that of Ba.

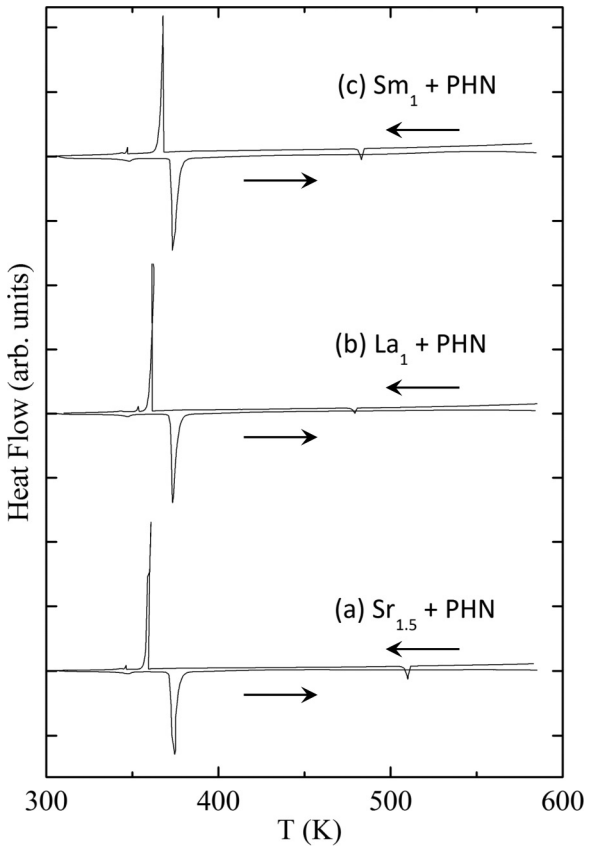

FIG. 9. DSC traces for (a) $Sr_{1.5}$+PHN, (b) La_1+PHN, and (c) Sm_1+PHN. The arrows indicate scan direction of heating and cooling. It is apparent that no reactions occur at heating temperatures lower than the melting points of Sr, La, and Sm, respectively.

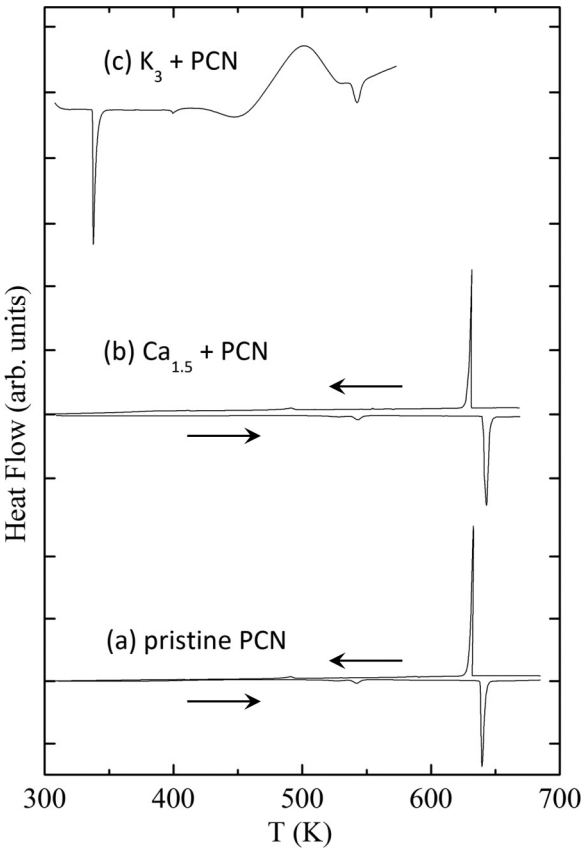

FIG. 10. DSC traces for (a) pristine PCN, (b) $Ca_{1.5}$+PCN, and (c) K_3+PCN. The arrows indicate scan direction of heating and cooling. There is no reaction in the case of Ca and PCN at heating temperatures below the melting point of Ca metal.

C. PCN with alkali and alkaline earth metal

We also measured DSC thermograms for PCN mixed with K or Ca (Fig. 10). Only an endothermic peak corresponding to the melting point of PCN was observed for PCN with Ca. On the other hand, in the case of PCN with K, a broad exothermic peak to be ascribed to a reaction appeared at around 500 K. In order to obtain more detailed information about the reaction processes, the annealing time dependence of XRD measurements was studied. The XRD profiles of K_3+PCN are shown as a function of annealing time in Fig. 11. After mixing PCN with K, a small peak for pristine PCN and free K metal appeared in the XRD profile. Annealing was repeated many times according to the conditions described in the previous report [1]. After 5 h annealing, a sharp peak derived from free K metal completely disappeared, but at the same time KH gradually formed. The XRD profiles can be explained by considering pristine PCN, free K metal, hydride KH, and new broad peaks with small intensity. The reaction finished within an annealing time of 5–10 h under this reaction condition. We also checked whether superconductivity appears using the same XRD capillary (Fig. 12), but no trace of superconductivity was detected above 2 K for more than 400 specimens of K_x (PCN) in two different laboratories.

We observed a mysterious behavior of magnetization for K_3 (PCN) as shown in Fig. 13(a). This behavior is similar to the reported one, which was previously assigned to the

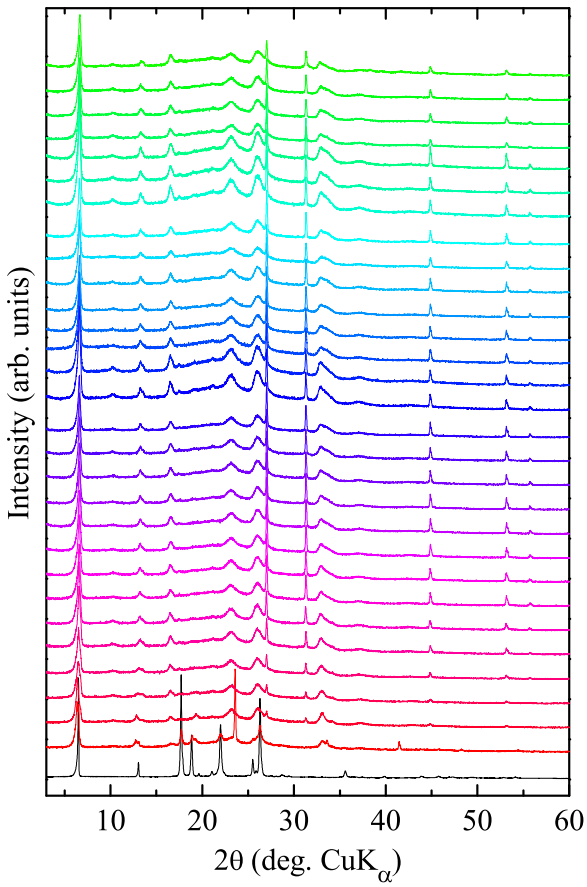

FIG. 11. (Color online) Annealing time dependence of XRD profiles for K_3+PCN. (From bottom to top): Pristine PCN, after mixing, and after 5, 10, 20, 40, 60, . . . , 540 h, respectively.

superconducting shielding curve of K_3 (PCN) by Mitsuhashi *et al.* [1]. The magnetization showed a sharp change and had a very large paramagnetic value in contrast to the conventional molecular superconductors. It can easily be understood that this is not the superconducting transition, because the data of

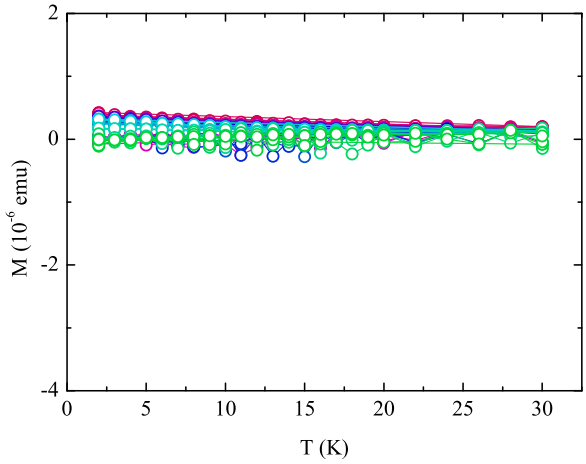

FIG. 12. (Color online) Temperature dependence of magnetization for K_3+PCN with increasing annealing time using XRD capillary under an applied magnetic field (H) of 10 Oe. Increases in annealing time were shown by color change from red (after mixing) to green (340 h).

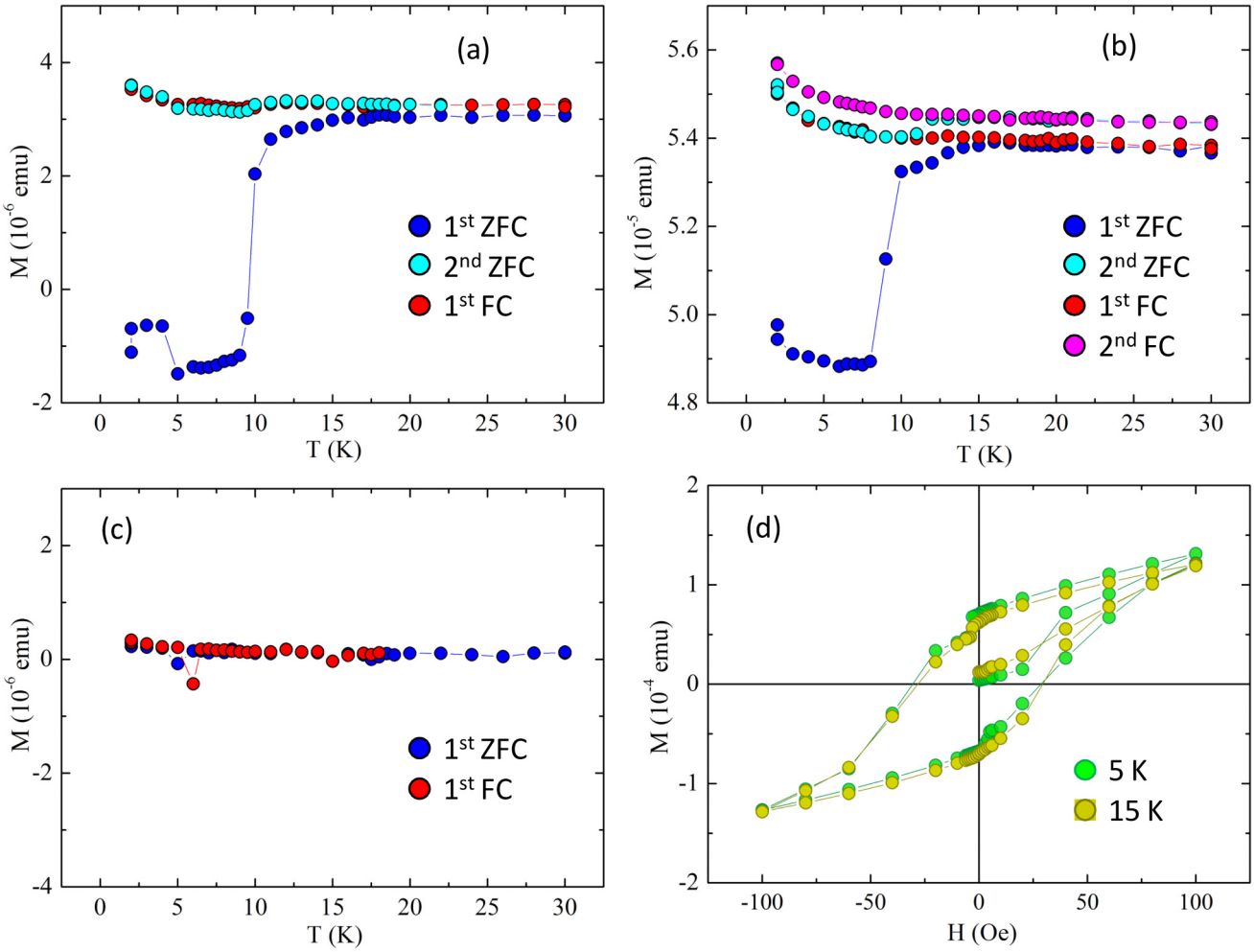

FIG. 13. (Color online) (a) Temperature dependence of magnetization for the nominal composition of K_3 (PCN) under ZFC and FC conditions. Measurements were carried out under $H = 5$ Oe. Also shown is the magnetization for (b) the removed ferromagnetic fragments by using magnet and (c) the specimen after removing the ferromagnetic fragments and (d) the magnetic field dependence of magnetization for the ferromagnetic fragments.

the second ZFC are almost the same as those of the first field cooling (FC). Its origin should be attributed to a ferromagnetic component as can clearly be shown by a hysteresis curve in Fig. 13(d). It is important to note that this behavior completely disappeared when the ferromagnetic fragments were removed by magnet as shown in Fig. 13(c).

A magnetic measurement apparatus has a general feature that small residual magnetic field remains even when the apparatus is used under a zero field setting. In a SQUID magnetometer, when a sample is cooled down under $H = 0$ Oe setting, a weak residual magnetic field is actually applied to a sample. When the sample does not contain a ferromagnetic impurity, this feature does not cause any wrong consequences. However, when a ferromagnetic impurity is involved in the sample, small grains or domains consisting of ferromagnetic spins with random orientation immediately align to the same direction as the residual magnetic field. The direction of the induced magnetic moment depends on the starting point on the ferromagnetic hysteresis curve of the sample, and importantly in this case the direction of the induced magnetic moment is minus in sign. Once the magnetic domains of the ferromagnetic impurities align to one direction, the magnetic moment survives until a static magnetic field reaches about 30 Oe in the present case as shown in Fig. 13(d). Consequently, when one measures the sample under the ZFC with $H <$ 30 Oe, a signal, misinterpreted to a superconducting signal, is observed. This signal is of course an artifact and not a true superconducting signal.

IV. SUMMARY

The reactions of PHN and its geometrical isomer AN with K were thermodynamically studied by using DSC and XRD measurements. There was a remarkable difference in reactivity between PHN and AN with K. Thermal treatment of K_3 (PHN) at 473 K led to molecular decomposition. Finally, only KH and unidentifiable by-products were obtained. No stable doped phases were observed in the K-PHN system. On the other hand, a stable doped phase was clearly observed in the K-AN system. The thermodynamic stability of AN in the reaction process was higher than that of PHN, which is opposite to the relative stabilities in their ground states

reported by theoretical calculations. No signals corresponding to superconductivity were observed for K_x (PHN) with $x =$ 1–3 above 2 K. These results completely contradict to the previous reports. The presence of superconducting states in M_x (PHN/PCN) (M = alkali, alkaline earth, rare earth metal) is extremely questionable.

ACKNOWLEDGMENTS

This research was supported by Science Research on Priority Areas of New Materials Science using Regulated Nano Spaces, Tohoku University Global Center of Excellence (GCOE) program "Weaving Science Web beyond Particle-Matter Hierarchy", and a Grant in Aid for Scientific Research and World Premier International Research Center Initiative (WPI) from the Ministry of Education, Culture, Sports, Science and Technology (MEXT) of Japan. This work was partly supported by the Joint Studies Program: No. 252 and No. 630 of the Institute for Molecular Science (S. H.) and by the Nanotechnology Platform Program: No. B107, No. S-13-MS-0004, No. S-13-MS-1041, and No. S-14-MS-1046 (Molecule and Material Synthesis) of MEXT (M.K. and S.H.).

[1] R. Mitsuhashi, Y. Suzuki, Y. Yamanari, H. Mitamura, T. Kambe, N. Ikeda, H. Okamoto, A. Fujiwara, M. Yamaji, N. Kawasaki, Y. Maniwa, and Y. Kubozono, Nature (London) **464**, 76 (2010).

[2] X. Wang, R. Liu, Z. Gui, Y. Xie, Y. Yan, J. Ying, X. Luo, and X. Chen, Nat. Commun. **2**, 507 (2011).

[3] T. Kosugi, T. Miyake, S. Ishibashi, R. Arita, and H. Aoki, Phys. Rev. B **84**, 020507 (2011).

[4] T. Kato, T. Kambe, and Y. Kubozono, Phys. Rev. Lett. **107**, 077001 (2011).

[5] G. Giovannetti and M. Capone, Phys. Rev. B **83**, 134508 (2011).

[6] M. Kim, B. I. Min, G. Lee, H. J. Kwon, Y. M. Rhee, and J. H. Shim, Phys. Rev. B **83**, 214510 (2011).

[7] P. L. de Andres, A. Guijiarro, and J. A. Verges, Phys. Rev. B **83**, 245113 (2011).

[8] M. Casula, M. Calandra, G. Profeta, and F. Mauri, Phys. Rev. Lett. **107**, 137006 (2011).

[9] P. Cudazzo, M. Gatti, and A. Rubio, Phys. Rev. B **86**, 195307 (2012).

[10] A. Ruff, M. Sing, and R. Claessen, Phys. Rev. Lett. **110**, 216403 (2013).

[11] K. Teranishi, X. He, Y. Sakai, M. Izumi, H. Goto, R. Eguchi, Y. Takabayashi, T. Kambe, and Y. Kubozono, Phys. Rev. B **87**, 060505 (2013).

[12] T. Kambe, X. He, Y. Takahashi, Y. Yamanari, K. Teranishi, H. Mitamura, S. Shibasaki, K. Tomita, R. Eguchi, H. Goto, Y. Takabayashi, T. Kato, A. Fujiwara, T. Kariyado, H. Aoki, and Y. Kubozono, Phys. Rev. B **86**, 214507 (2012).

[13] H. Okazaki, T. Wakita, T. Muro, Y. Kaji, H. Mitamura, N. Kawasaki, Y. Kubozono, Y. Yamanari, K. Kambe, T. Kato, M. Hirai, Y. Muraoka, and T. Yokoya, Phys. Rev. B **82**, 195114 (2010).

[14] H. Okazaki, T. Jabuchi, T. Wakita, T. Kato, Y. Muraoka, and T. Yokoya, Phys. Rev. B **88**, 245414 (2013).

[15] B. Mahns, F. Roth, and M. Knupfer, J. Chem. Phys. **136**, 134503 (2012).

[16] M. Caputo, G. Di Santo, P. Parisse, L. Petaccia, L. Floreano, A. Verdini, M. Panighel, C. Struzzi, B. Taleatu, C. Lal, and A. Goldoni, J. Phys. Chem. C **116**, 19902 (2012).

[17] Y. Kubozono, H. Mitamura, X. Lee, X. He, Y. Yamanari, Y. Takahashi, Y. Suzuki, Y. Kaji, R. Eguchi, K. Akaike, T. Kambe, H. Okamoto, A. Fujiwara, T. Kato, T. Kosugi, and H. Aoki, Phys. Chem. Chem. Phys. **13**, 16476 (2011).

[18] Q.-W. Huang, G.-H. Zhong, J. Zhang, X.-M. Zhao, C. Zhang, H.-Q. Lin, and X.-J. Chen, J. Chem. Phys. **140**, 114301 (2014).

[19] G. Vernadsky, Russian Rev. **28**, 37 (1969).

[20] M. Fujita, K. Wakabayashi, K. Nkada, and K. Kusakabe, J. Phys. Soc. Jpn. **65**, 1920 (1996).

[21] K. Kusakabe and M Maruyama, Phys. Rev. B **67**, 092406 (2003).

[22] H. S. Chen, A. R. Kortan, R. C. Haddon, and N. Kopylov, J. Phys. Chem. **97**, 3088 (1993).

[23] J. Trotter, Acta. Cryst. **16**, 605 (1963).

[24] A. Charlesby, G. Finch, and H. Willman, Proc. Phys. Soc. **51**, 479 (1939).

[25] Q. T. N. Phan, S. Heguri, Y. Tanabe, H. Shimotani, T. Nakano, Y. Nozue, and K. Tanigaki, Dalton Trans. **43**, 10040 (2014).

[26] Q. T. N. Phan, S. Heguri, Y. Tanabe, H. Shimotani, and K. Tanigaki, Euro. J. Inorg. Chem. **2014**, 4033 (2014).

[27] D. Biermann and W. Schmidt, J. Am. Chem. Soc. **102**, 3163 (1980).

[28] X. F. Wang, Y. J. Yan, Z. Gui, R. H. Liu, J. J. Ying, X. G. Luo, and X. H. Chen, Phys. Rev. B **84**, 214523 (2011).

[29] S. Heguri, Q. T. N. Phan, Y. Tanabe, and K. Tanigaki, Phys. Rev. B **90**, 134519 (2014).

[30] X. F. Wang, X. G. Luo, J. J. Ying, X. J. Xiang, S. L. Zhang, R. R. Zhang, Z. H. Zhang, Y. J. Yan, A. F. Wang, P. Cheng, G. L. Ye, and X. H. Chen, J. Phys.: Condens. Matter. **24**, 345701 (2012).

[31] G. A. Artioli, F. Hammerath, M. C. Mozzati, P. Carretta, F. Corana, B. Mannucci, S. Margadonna, and L. Malavasi, Chem. Commun. **51**, 1092 (2015).